Optimization of the Compression (Injection/Compression) Molding Process Using Numerical Simulation

Bruce A. Davis
The Madison Group: Polymer Processing Research Corporation
Madison, Wisconsin

Richard P. Theriault
Tim A. Osswald
Polymer Processing Research Group
University of Wisconsin-Madison
Madison, Wisconsin

ABSTRACT

The increasing requirements on auto makers to reduce both the cost and weight of passenger vehicles as well as meet ever more restrictive government regulations make the use of fiber reinforced plastics very attractive. In particular, the use of thermoset composites, such as SMC and BMC, have been used for years by the major auto makers to produce high quality, strong, stiff, and lightweight body panels. Increasingly, it is being used for more structural components throughout the vehicle. However, the use of fiber filled thermoset composites is not limited to the automotive industry. It is also extensively used in electronic components, sports equipment, and general consumer goods. Accordingly, the need to be able to design these molded parts and to predict the complex behavior during manufacture and in service is paramount to reducing the time from concept to production.

This paper introduces a finite element based simulation program that allows the entire molding process, including mold filling, fiber orientation, heat transfer, cure, residual stress and warpage, to be simulated on the computer rather than by experimental prototyping. The software allows designers and engineers to determine product performance during the design stage before the tooling needs to be manufactured. Then, by modifying the design and process with the computer, part optimization can be accomplished prior to building the mold.

The paper discusses the models and methods implemented by the simulation program along with the accompanying assumptions. The results of the simulation are compared with experimental results for a variety of parts. This paper then highlights a case study of an injection/compression molded component showing how the simulation can be used as a design optimization tool.

INTRODUCTION

The compression molding process has been widely used to produce fiber reinforced thermoset composite parts. The molding of sheet molding compound (SMC) has, for years, been used to produce automotive body panels and structural components. However, the molding of SMC is limited in production rates because it typically requires a dedicated press operator to place the raw material in the mold. As an alternative, the injection/compression (I/C) process can be used to increase production rates because it does not require the manual cutting and placement of SMC. However, because the raw material must pass though a gate during the injection phase, SMC cannot be used in the I/C process. Instead, materials such as bulk molding compound (BMC) or vinyl esters are used. These materials typically have shorter glass fibers than SMC and accordingly exhibit lower structural properties. Additionally, the I/C process is considerably more difficult to simulate than the compression molding process and must be examined in more detail.

Because the injection/compression molding process is more complicated than the straight compression molding process, there are certain additional inputs that are required to calculate the solutions. Such properties as the volumetric flow rate of the injected material, the gate location and size, and the initial tool gap height all need to be properly defined before the mold filling process can be calculated. As the name suggests, the injection/compression molding process is a two stage operation. Although the actual details of the process can be quite complex, from the standpoint of simulation it can be described as shown in Fig. 1. Initially, the tool is closed enough to engage the shear edges and seal off the mold. Next, enough material to volumetrically fill the part is directly injected into the mold, the injection gate valve then closes off the mold, and the compression phase of the process begins. Now, the process continues exactly like compression molding with the tool closing until the part is completely filled and cured sufficiently to de-mold.

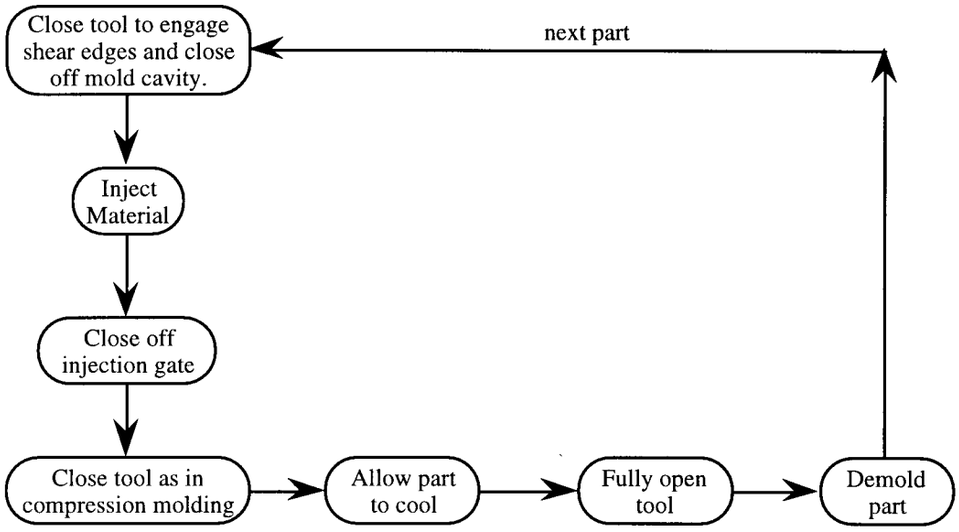

Figure 1 - Injection/Compression (I/C) molding process cycle

In order to simulate this process, a general understanding of the nomenclature used above is required. Initially, the tool is closed sufficiently such that the shear edges have engaged and the cavity is closed to prevent leakage. This state is illustrated in Fig. 2. Here, only a portion of the tool is shown where the shear edges and support surfaces are removed for clarity. Here, the *Initial Injection Height* is defined as the total gap height between the mold halves at the injection stage.

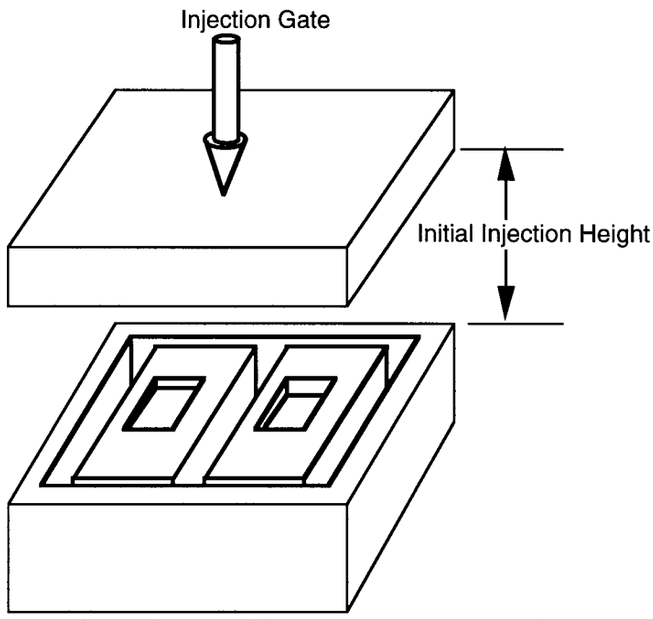

Figure 2 - Tool schematic during the injection phase of the I/C process

At this point, the material is injected into the mold cavity through the injection gate. After a sufficient amount of material has been injected to volumetrically fill the part, the mold is closed to the *Final Compressed Height*, as shown in Fig. 3. This closing phase is identical to the standard compression molding process, except instead of placing the SMC into the mold the material has been placed by the injection phase.

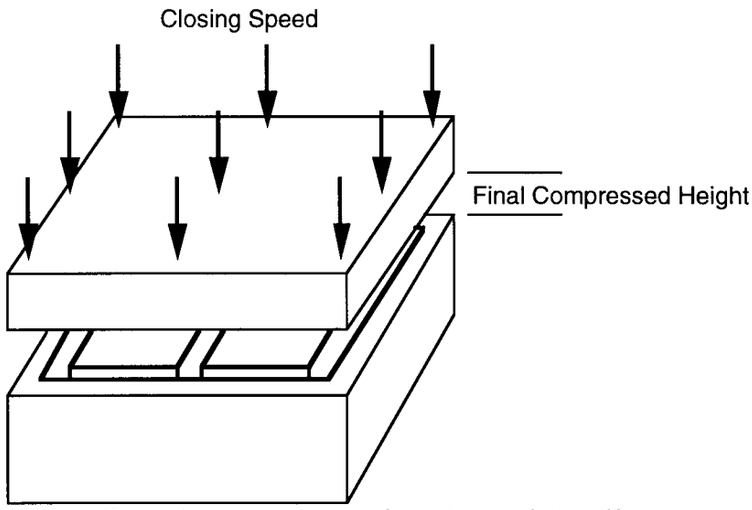

Figure 3 - Tool schematic during the compression phase of the I/C process

Differences from Compression Molding

As evidenced from the prior discussion, there are several substantial differences between the injection/compression molding of BMC and the standard compression molding process. The first difference in the process is that the tool is now initially separated at a fixed gap to ensure that the shear edges are engaged to seal the mold cavity. The distance that the mold is backed-up from the final compressed height is referred to as the *Backup Height.* Using the notation from Figs. 2-3, the backup height can be defined as

Backup Height = Initial Injection Height - Final Compressed Height. (1)

The backup height can be highly instrumental in the formation/avoidance of knitlines. For the standard compression molding process the initial charge location is well defined, since individual layers of SMC are placed in the mold cavity at the start of the process. However in the injection/compression process the initial charge location is determined by the outcome of the injection phase. Since the injection phase serves to locate the initial charge location for the compression phase, it is paramount that the proper region be filled. If the backup height is large, then only a small area of the mold cavity will be filled by the initial injection of material. However, as the backup height is decreased, the portion of mold coverage from initial injection increases. Often it is more convenient to understand this concept by taking the limit in which the backup height is 0. Here, the initial injection height is exactly equal to the final compressed height and a pure injection process occurs (identical to the injection molding process). In this case, it should be obvious that the injected material will completely fill the mold cavity—100% mold coverage. However, as the backup height is increased, and the volume of injected material remains constant, it follows that lower percentages of mold coverage will be obtained. Since the backup height directly affects the mold coverage area from the initial injection, it can greatly affect the outcome of the flow analysis.

Equally important to the resulting mold filling is the gate location. Unlike compression molding, where the charge location can be varied once the tool has been machined, the injection/compression molding process must have its gate location defined at build time. The gating location can either be a simple single circular gate, multiple gates, or edge gates along the entire length of a part. There are also additional specialty gates that may conform to certain mold features and have non-standard shapes and dimensions. Obviously, the placement of the gate(s) can dramatically affect the mold filling and knitline formation in the part.

In addition to the location and number of gates, the individual sizes and injection flow rate can also alter the flow field. If the gate cross sectional area is too small, then detrimental fiber damage can occur during injection. Also, if the gate area is too small for the given injection rate, excessive heating and damage can occur. For multiple gates or edge gates, there also exists the possibility for non uniform injection rates. If the runner system is not properly designed, then individual gates or regions can experience different flow rates during injection. This can, in turn, lead to knitlines or improper mold filling patterns.

There also exists, in injection/compression molding, an initial fiber orientation in the material after the injection phase. In standard compression molding, the SMC sheets of raw material are manufactured in such a way as to produce a nearly random fiber orientation distribution. However, in the injection/compression process, the flow during the injection phase tends to orient the fibers in the circumferential direction. Because the injection process produces a radial expansion flow outward from the gate, the fibers show a proclivity for orientation in the tangential direction. However, as obstacles in the mold cavity alter the flow field, the fiber orientation becomes more complex. Therefore, the initial fiber orientation after the injection phase can greatly affect the material properties in the final part. These phenomena will be further discussed is more detail in this paper.

MATERIALS

Bulk molding compound (BMC) is a glass fiber reinforced composite material based on unsaturated polyester; a resin that can be formulated in an almost infinite number of ways. As shown in Table 1, BMC is a totally integrated composite which incorporates all of the reinforcement, resin, fillers, chemical thickeners, catalysts, mold release agents and other ingredients (Barone and Caulk, 1979).

Table 1. Composition of bulk molding compound.

Resin		27.35 %
Unsaturated Polyester	10.50 %	
Low Shrink Additive	3.45 %	
Styrene Monomer	13.40 %	
Filler (Calcium Carbonate)		40.70%
Thickener (Magnesium Oxide)		0.70%
Initiator		0.25%
Lubricant (Zinc Stearate)		1.00%
Glass Fibers (12 mm long)		30.00%

When subjected to elevated temperatures, the crosslinking reaction of unsaturated polyesters is carried out via copolymerization between the low molecular weight unsaturated polyester prepolymer and the styrene monomer as shown in Fig. 4. The reaction is slowed and eventually terminated as the rate of propagation of the reacting chains is in competition with the availability of reactive sites. The mechanical and thermomechanical properties of thermoset resins can be directly correlated to the reaction kinetics.

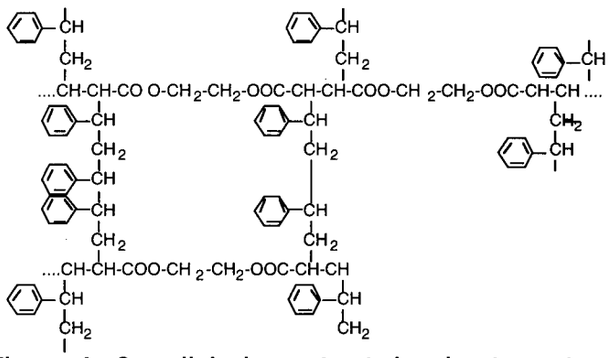

Figure 4. Crosslinked unsaturated polyester network

THEORETICAL BACKGROUND OF MOLD FILLING

For the injection/compression molding process the mold filling stage is broken into two distinct physical driving forces. The initial injection phase is governed by a flow rate controlled gate where raw material is injection into the mold. This initial injected flow field is dominated by a uniform radial expansion flow. After a sufficient volume of material has been injected, the compression phase begins to squeeze the material to completely fill the mold. Although the two phases are substantially different, they can be described by the same material flow model. Then, with proper application of boundary conditions, the solution to the mold filling stage can be entirely simulated with a numerical approach.

During the processing of filled thermoset polymers the material deforms uniformly through the thickness with slip occurring at the mold surface. The flow phenomenon of fiber filled thermoset materials has been well documented by Osswald (1987) and can be numerically modeled by the control volume approach (CVA). Since the typical automotive component has a much larger planar dimension than the thickness of the part, the shell Galerkin finite element method based on the models of Barone & Caulk (1985) can be used. The assumptions of the model are as follows:

1. The mold is thin with respect to the surface dimension.
2. The mold closing speed for the compression phase is $(-\dot{h})$.
3. The molding compound is treated as an incompressible isotropic viscous fluid.

4. The non-isothermal conditions in the mold form a lubricating layer at the mold surfaces and the material is dominated by plug flow. This plug flow can be described by a lubrication analogy with kinemetic friction.
5. There is no leakage at the edges of the mold.

The Barone and Caulk flow model can be described in the following two equations. Equations 2-3 show the pressure, P, in the mold as a function of the flow conductance, S, and the mold closing speed, $\dot{h}$. The flow conductance is further defined in Eq. 3 to be a function of the mold gap height, h, and the kinematic friction factor, K_h, between the material and mold surfaces.

$$\frac{\partial}{\partial x}\left(S\frac{\partial P}{\partial x}\right)+\frac{\partial}{\partial y}\left(S\frac{\partial P}{\partial y}\right)=\dot{h} \tag{2}$$

$$S=\frac{h^2}{2K_h} \tag{3}$$

Developing finite element equations for the Newtonian non-isothermal problem is straightforward since a functional whose minimization corresponds to the solution of Eq. 2 is known. This leads to a set of linear finite element equations which can be summarized in Eq. 4. Here, the element stiffness matrix $[k]_e$ multiplied by the element pressures $\{P\}_e$ is equal to the element forcing functions $\{f\}_e$ generated by the flow conductance, the mold closing speed, and the flow rate from the injection gate.

$$[k]_e\{P\}_e=\{f\}_e \tag{4}$$

The element equations can be assembled to create a global stiffness matrix and force vector for a specific part geometry. After modifying the global stiffness matrix and forcing vector in order to ensure that the boundary conditions at the free flow front have been met, the equations are solved for nodal pressures. These nodal pressures can then be used in the CVA to predict flow between elements and the mold filling process.

For the injection/compression molding process in particular, the mold filling process is broken into two distinct phases. In the first, the mold is held stationary where $\dot{h}=0$ but material is injected through the gate. Here, the flow rate is applied as a nodal source point where the force is directly related to the volumetric flow rate through the gate. This process continues until a sufficient amount of material has been injection to volumetrically fill the part. Then, the injection gate valve is closed and the mold begins to squeeze the material to completely fill the mold. In the second phase, the forcing function is now related to the mold closing speed $\dot{h}$ and the flow conductance from the Barone and Caulk model.

THEORETICAL BACKGROUND OF FIBER ORIENTATION

Reinforcing fibers become oriented by flow during processing. Fiber orientation is a major cause of warpage in chopped fiber reinforced composites. For many years, the flow induced fiber orientation was treated as an undesirable effect of processing. Much effort has been placed in producing BMC parts with random orientation of fibers to have isotropic mechanical properties. However, by controlling the fiber orientation pattern, one might get the desired characteristics of the material, and this is one reason for research on the prediction and control of the fiber orientation in reinforced polymers.

The governing equation which describes the fiber rotation due to the flow field is the fiber density continuity equation is expressed as

$$\frac{\partial \Psi}{\partial t}=-\frac{\partial}{\partial \varphi}(\Psi\dot{\varphi}) \tag{5}$$

where φ is the orientation angle, Ψ represents the orientation distribution function, and $\dot{\varphi}$ is the angular velocity of the fiber. The Folgar-Tucker model (1984) can be used to describe the flow induced fiber orientation accounting for fiber-fiber interaction as

$$\dot{\varphi} = -\frac{C_I \dot{\gamma}}{\Psi}\frac{\partial \Psi}{\partial \varphi} - cs\frac{\partial v_x}{\partial x} - s^2\frac{\partial v_x}{\partial y} + c^2\frac{\partial v_y}{\partial x} + sc\frac{\partial v_y}{\partial y} \tag{6}$$

where C_I is the fiber-fiber interaction coefficient, $\dot{\gamma}$ is the magnitude of the strain rate tensor, and s and c are the $\sin\varphi$ and $\cos\varphi$, respectively.

The fiber orientation distribution effects both the elastic properties of the finished composite and the thermomechanical properties important in the development of shrinkage and warpage. Osswald and Tseng (1993) were able to successfully describe the elastic properties of an oriented composite with the use of the laminate analogy model (Halpin, 1969) and the thermomechanical properties with the Schneider's (1971) approximation.

There also exists, in injection/compression molding, an initial fiber orientation in the material after the injection phase. In standard compression molding, the SMC sheets of raw material are manufactured in such a way as to produce a nearly random fiber orientation distribution. However, in the injection/compression process, the flow during the injection phase tends to orient the fibers in the circumferential direction as shown in Fig. 5. Because the injection process produces radial expansion flow outward from the gate, the fibers show a proclivity for orientation in the tangential direction. However, as obstacles in the mold cavity alter the flow field, the fiber orientation becomes more complex. Therefore, the initial fiber orientation after the injection phase can greatly affect the material properties in the final part.

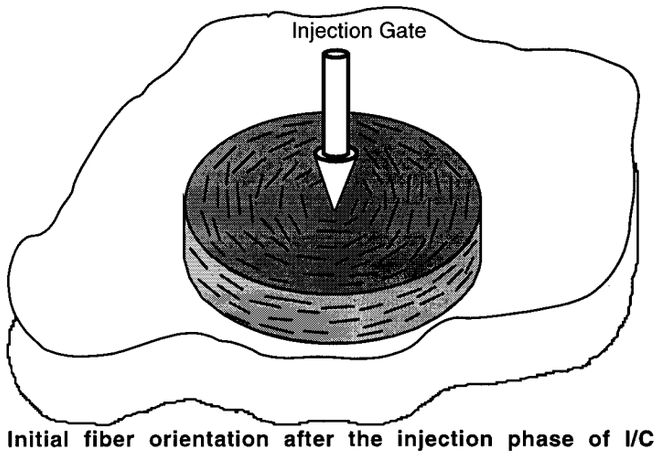

Figure 5. Initial fiber orientation after the injection phase of I/C molding

THEORETICAL BACKGROUND OF CURE KINETICS

The transformation of a reactive thermosetting liquid to a glassy solid generally involves two distinct macroscopic transitions: molecular gelation and vitrification. Molecular gelation is defined as the time or temperature at which covalent bonds connect across the network form an infinite three-dimensional network which gives rise to long range elastic behavior in the macroscopic fluid. Vitrification is when the glass transition temperature of the system rises to the cure temperature and when further reaction is prohibited or is dramatically reduced.

The curing reaction of thermally cured thermoset resins is not immediate, thus the blend can be stored for a short period of time before use. However, at higher temperatures, the curing reaction is

accelerated and can generate an appreciable exotherm. The generalized time-temperature-transformation (TTT) cure diagram developed by Wisanrakkit and Gillham (1990) is used to relate the material properties of thermoset as a function of time and the curing temperature as shown in Fig. 6.

There are several distinct regions of matter on the TTT diagram; liquid, sol-gel rubber, gel-rubber, sol-gel glass, gel-glass, sol-glass and char. Isothermal heating of a sample is represented by a horizontal line on Fig. 6, thus the sample will pass through a particular region depending on the initial temperature chosen. The resin will not cure and remain in an ungelled vitrified (or solid) state if stored below Tg_0 due to the immobilization of the reactive species in the glassy state. Below ${}_{gel}Tg_0$, the resin is capable of slight cross linking in the liquid state, however, reaction rates are so slow that at these isothermal temperatures, a very small conversion is achieved by the time the resin vitrifies and thus will remain in an ungelled state. Above Tg_∞, the resin will not vitrify though high conversions are reached, however, with long cure times, chain degradation at the elevated temperatures may develop as a competitive reaction that will diminish the degree of conversion. Of practical consideration, the region between ${}_{gel}Tg_0$ and Tg_∞ is of most use to processors. As shown by the "S" shaped vitrification curve, higher isothermal temperatures increase the time to reach the gelled glass state. This is due to the favorable steric association for propagation of the resin due to the decrease in viscosity and the increase in reaction rates as a function of temperature (Odian, 1991). At higher temperatures the time to vitrification obtains a minimum value due to the competing effects between the reaction rates and the consumption of the reactants.

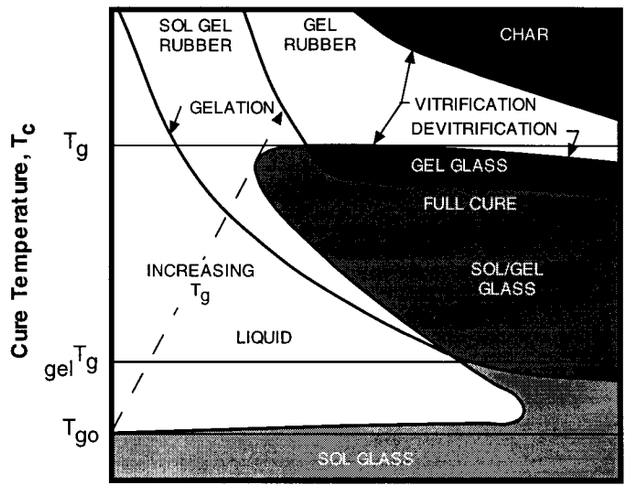

Figure 6. Time-Temperature-Transition (TTT) Diagram

The injection/compression molding process for BMC begins when the material is injected inside a heated mold. The mold is then closed, forcing the material to flow over the mold's surface. An order of magnitude analysis shows that for thin parts the heat conduction across the thickness is much larger than the conduction along the larger dimensions of the part (Barone and Caulk, 1979) and (Osswald, 1991). Hence, the energy equation reduces to a one dimensional equation which can be solved by the finite difference method. However, when dealing with thermosetting polymers, the energy equation has an extra term, $\dot{Q}$, that deals with the exothermic curing reaction. This heat generation due to cure can be expressed as

$$\dot{Q} = Q_t \frac{dc}{dt} \tag{7}$$

where c is the degree of cure, Q_t is the total amount of heat released during the reaction. The degree of cure is assumed to be proportional to the number of bonds formed curing crosslinking and that each bond releases the same amount of heat. The rate of cure of an unsaturated polyester resin can be represented an autocatalytic reaction rate as

$$\frac{dc}{dt} = (d_1 + d_2 \cdot c^m)(1-c)^n \tag{8}$$

where the terms d_1 and d_2 contain the temperature dependence of the curing reaction rate as well as a diffusive term representing reactant consumption as the vitrification temperature is approached.

$$\frac{1}{d_1} = \frac{1}{a_1 \cdot e^{-E_1/RT}} + \frac{1}{a_d \cdot e^{-E_d/RT} \cdot e^{-b/f}} \tag{9a}$$

$$\frac{1}{d_2} = \frac{1}{a_2 \cdot e^{-E_2/RT}} + \frac{1}{a_d \cdot e^{-E_d/RT} \cdot e^{-b/f}} \tag{9b}$$

where R is the gas constant, f is the fractional free volume, and E_1, E_2, E_d, a_1, a_2, a_d, and b are constants which can be obtained by fitting Eqs.(9.a-b) to data measured in a differential scanning calorimeter. More detail on the model is given in (Simon and Gillham, 1993) and the solving procedure in (Tseng, 1993).

THEORETICAL BACKGROUND OF MATERIAL PROPERTIES DURING CURE

The occurrence in these systems of differently activated and kinetically distinct reactions affects the chemorheology of the cure, gelation, and vitrification processes. In fact, the gelation and vitrification phenomena, which usually occur in two distinct stages of the processing, such as the initial polymerization and final postcure, may strongly influence the thermoset molecular morphology and hence the material properties.

Flory (1953) used a statistical approach to derive an expression for predicting the extent of reaction at gelation. The statistical approach assumes that the reactivity of all functional groups of the same type is the same and independent of molecular size. It is further assumed that there are no intramolecular reactions between functional groups on the same molecule. According to Flory's theory of gelation, a crosslinked system will gel molecularly when its fractional conversion, c, reaches a constant critical value given by

$$c_{gel} = \frac{1}{[r + rp(f-2)]^{1/2}} \tag{10}$$

where f is the functionality of the crosslinking groups, r is the molar ratio of reacting function groups, and p is the fraction of reactive sites of one type in the branching units with the same type.

For a system exhibiting a unique one-to-one relationship between the glass transition temperature and conversion, Di Benedetto's (1987) equation is one of the easiest approaches for stoichiometric ratios to express this relationship using only a single parameter model.

$$T_g = T_{g_o} + \frac{\left(T_{g_\infty} - T_{g_o}\right)\lambda c}{1-(1-\lambda)c} \tag{11}$$

where T_{g_o} is the glass transition temperature of the monomer, T_{g_∞} is the glass transition temperature of the fully reacted network, λ is a structure dependent parameter theoretically equated to $\Delta C_{p_\infty}/\Delta C_{p_o}$. The values of ΔC_{p_∞} and ΔC_{p_o} are the differences in the heat capacity between the glassy and rubbery state for the fully cured network and monomer, respectively.

Between the gelation and vitrification points, the material properties are governed by competing mechanisms between chemical hardening and viscoelastic relaxation (Bogetti and Gillespie, 1989 and 1990). However, Hahn and Kim (1989) have reported a linear–like correlation between the material properties and degree of cure.

THEORETICAL BACKGROUND OF SHRINKAGE AND WARPAGE

Once the curing reaction exceeds the gel point, residual stresses start to build up. The governing equations for the stress analysis used during solidification and part removal are derived using the principle of virtual work. The principle states that for a body which is in static equilibrium, the virtual internal work created by the stresses and the virtual strains, equals the virtual external work done by the external forces and the virtual displacements. Equating the internal and external virtual work results in

$$\int_V \{\delta\varepsilon\}^T \{\sigma\} dV = \{\delta u\}^T \{f\} \tag{12}$$

where $\{\delta\varepsilon\}$ are the virtual strains, $\{\sigma\}$ the stresses, $\{\delta u\}$ the virtual displacements and $\{f\}$ the externally applied forces. The stresses in the model are represented as a function of local strain and the residual stress $\{\sigma_o\}$

$$\{\sigma\} = [E]\{\varepsilon\} - [E]\left\{\varepsilon_o^{tot}\right\} + \{\sigma_o\} \tag{13}$$

In Eq. (13) the material tensor $[E]$ is anisotropic and dependent on the local degree of cure and $\left\{\varepsilon_o^{tot}\right\}$ is the total internal strains that occur due to curing, cooling or heating during a time step. Two kinds of internal strains should be included in simulating the thermomechanical behavior of thermoset composites. One is thermal strain caused by a temperature change and the other is curing strain resulting from crosslinking polymerization of thermoset resins. The thermal strains can be represented in terms of temperature change and thermal expansion coefficients.

$$\{\varepsilon_o\}^{Thermal} = \Delta T\left\{\alpha_{xx}\ \alpha_{yy}\ \alpha_{zz}\ \alpha_{xy}\ 0\ 0\right\} \tag{14}$$

Tseng and Osswald (1993) neglected the effect of the shrinkage due to curing, since warpage in thin sections is mainly caused by the difference between thermal expansion coefficients of the fiber and matrix. However, for thicker sections this may not be overlooked since the shrinkage due to curing is the main cause of internal cracking.

Due to the large fiber–length/part–thickness ratio, most fibers in BMC parts are oriented in the planar direction. This leads to higher thermal expansion coefficients in the thickness direction as compared to those in the surface direction. It is well known that angular distortion can occur when forming a curved–sectioned part, a consequence of the anisotropy of the composites, as shown in Fig. 2. This anisotropy induced curvature change is generally called the "spring–forward" effect. O'Neill

and Rogers (1988) reported the analytical solution for a cylindrical shell with three–dimensional anisotropies that exist in composite laminates. Their approach indicated that through–thickness thermal strains, caused by different thermal expansion coefficients, could lead to an angle distortion of a cylindrical shell experiencing a temperature change. As demonstrated in Fig. 2, when a curved part experiences a temperature change of ΔT, the curved angle, θ, will change by $\Delta\theta$ (Tseng, 1993). Sometimes only a slight angle change can cause significant warpage in a larger part. Therefore, it is of great importance to take this effect into account .

Unfortunately, conventional thin shell element formulation neglects the stress through the thickness of the part since it is much smaller than the in–plane stresses. To account for the through–thickness warping effect the through–thickness stress distribution is approximated by a linear function. This allows the stress variations across the thickness of the part to be replaced by an equivalent moment, obtained by integrating the stress distribution through the thickness.

The simulation begins with the input of the part's geometry, initial conditions, process parameters and boundary conditions. Next, the steps mentioned above are executed. The calculations in the filling and curing stage are done in several time steps and since relaxation is neglected, the cooling stage is a single time step calculation.

CASE STUDY - ANALYSIS OF A VALVE COVER

Since all of the theory and models behind mold filling, fiber orientation, material evolution, and shrinkage and warpage are now available, the next step was to develop a simulation program to fully characterize the injection/compression molding process of fiber filled thermosets. By using the commercially available compression molding program, Cadpress, and developing new modules for filling and fiber orientation if the I/C process, the complete injection/compression molding process can now be numerically simulated.

In order to demonstrate the effectiveness of the simulation algorithm, a case study of the injection/compression molding of a valve cover is described in detail. For this study, the valve cover was initially compression molded using SMC. However, in order to increase production, it is desirable to switch the process over to injection/compression molding of BMC.

The initial charge layout for the compression molding process, shown in Fig. 7, gives the location of the SMC charge. This charge location gave good filling results with acceptable fiber orientation distributions throughout the part. Initially, it was proposed to place the gate in the center of the region that was charged with SMC. However, after the mold filling results were obtained, it was found that a knitline was unavoidable at the oil fill hole.

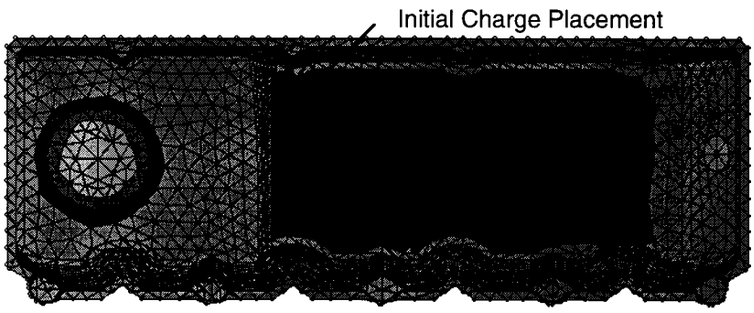

Figure 7. SMC charge placement for compression molding

The gate location, shown in Fig. 8, was initially chosen with the intent to produce approximately the same mold coverage as the charge of the compression molded SMC part in Fig. 7. It was thought that if the injection phase could transfer the raw material into the cavity in roughly the same position as the SMC sheets were placed, similar fiber orientation and stiffness would be

obtained. However, because of the rather thin region surrounding the oil fill knockout and the steep draft angles around the hole, a knitline was formed. The knitline, or weld line, formed on the downstream side of the oil fill hole because of the converging flow fronts flowing around the hole itself. Unfortunately, a knitline in this region compromised the structural integrity of the finished part and precluded this gating option as a viable manufacturing alternative.

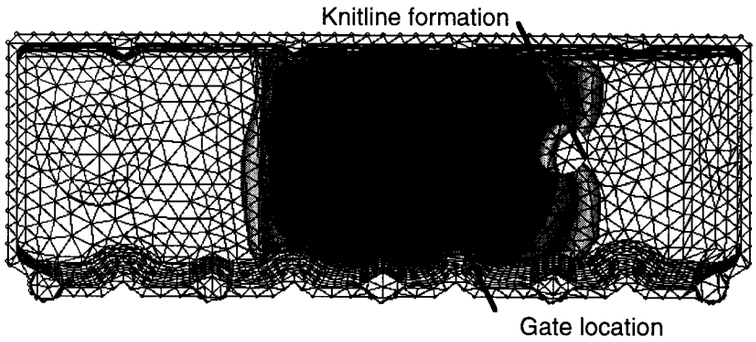

Figure 8. Flow pattern at the end of injection phase for I/C molding showing the initial injection gate location and presence of a knitline

In order to avoid the knitline around the oil fill hole, a second gating option was investigated. Here, the gate was placed in the center of the oil fill hole itself. As shown in Fig. 9, the resulting flow field at the end of the injection phase avoids any knitlines. The initial injected material also closely resembles the SMC charge placement shown in Fig. 7.

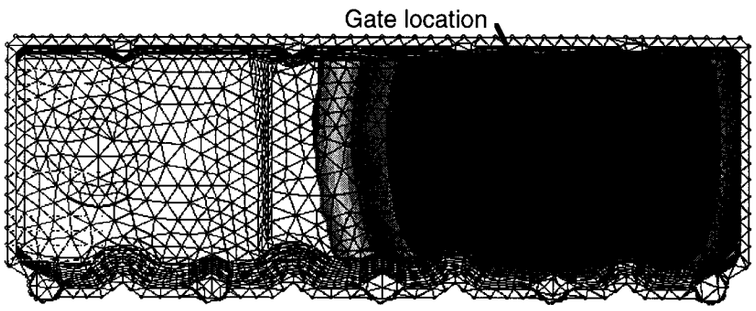

Figure 9. Flow pattern at the end of injection phase for I/C molding showing optimized injection gate location and no knitlines

Accordingly, the initial injection phase has also imparted a preferential fiber orientation distribution in the material. Figure 10 illustrates the effects of this initial fiber orientation from the injection phase. As the material flows outward from the gate, the radial expansion flow from injection causes the fiber to orient themselves in a tangential direction. However, as the figure shows, this tangential orientation is made more complex by the geometric features of the valve cover.

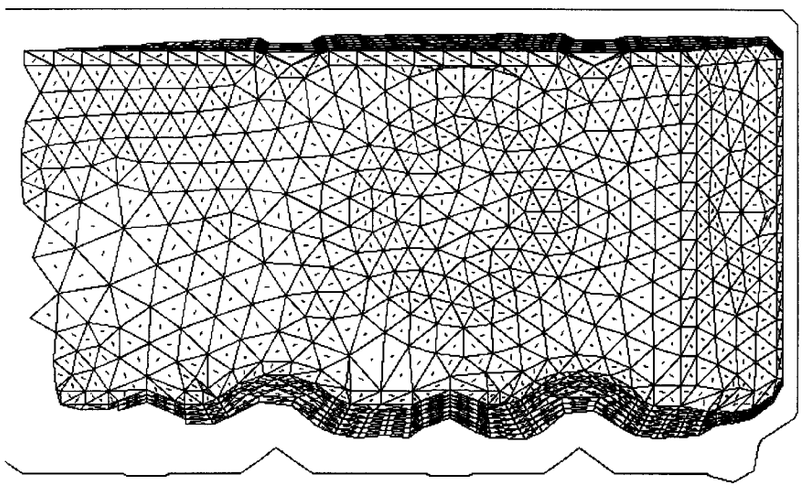

Figure 10. Flow induced fiber orientation the end of injection phase for I/C molding showing circumferential orientation

Finally, after the mold filling and fiber orientation have been fully calculated, the residual stress field during solidification can be computed. By using the aforementioned material models for the evolution of mechanical properties during cure, and solving the coupled energy and stress equations, the residual stress field can be obtained for the molded part. Upon de-molding this residual stress field causes the shrinkage and warpage as shown in Fig. 11. This figure shows a contour of the displacement field with a maximum deformation of only 1.2 mm.

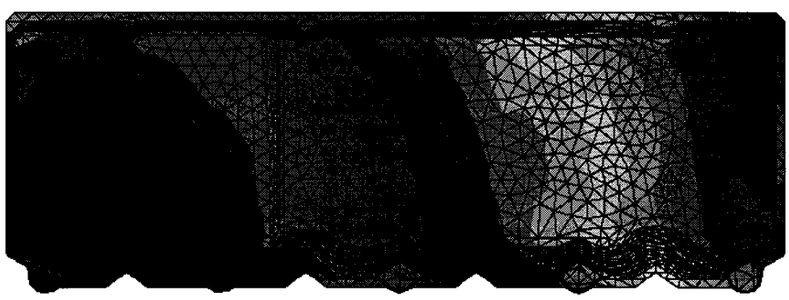

Figure 11. Shrinkage and warpage of the final molded part

CONCLUSION

Through the use of accurate material models, numerical methods, and computer simulation, it is now possible to fully calculate the injection/compression molding of fiber filled thermoset materials. As the case study illustrated, the full I/C molding process can be simulated and optimized via numerical modeling to yield a good part design. Since the I/C process requires more tool preparation to ensure that the injection gate is properly located, computer simulation also has the added advantage of being an extremely cost effective method to optimize both the process and part design.

REFERENCES

Barone, M. R. and D. A. Caulk., 1979, "The Effect of Deformation and Thermoset Cure on Heat Conduction in a Chopped-Fiber Reinforced Polyester during Compression Molding,"*Int.J.HeatMass Transfer,* Vol. 22, p.1021.

Barone, M.R., Caulk, D.A., "A Model for the Flow of a Chopped Reinforced Polymer Compound in Compression Molding," *J. Appl. Mech.*, 361-371 (1986).

DiBenedetto, A. T., 1987, *J. Polym. Sci. Polym. Phys.*, ed., Vol. 25, p.1949.

Bogetti, T. A. and J. W. Gillespie, 1989., "Process Induced Stress and Deformation of Thermoset Composites,"*21st Int. SAMPE Tech. Conf.*

Bogetti, T. A. and J. W. Gillespie, 1990, "Residual Stress and Deformation in Thick Laminated Composites Undergoing Chemical Hardening and Shrinkage," *45th SPI Conf. Proc.*, Vol. 19A, p.1.

Flory, P. J., 1953, *Principles of Polymer Chemistry*, Cornell University Press, Ithaca, New York.

Folgar, F. and C. L. Tucker, 1984, "Orientation Behavior of Fiber in Concentrated Suspensions," *J. Reinf. Plast. Comp.*, Vol. 3, p.98.

Halpin, J. C., 1969, "Stiffness and Expansion Estimates for Oriented Short Fiber Composites," *J. Comp. Mater.*, Vol. 3, p.732.

Kim, K. S. and H. T. Hahn, 1989, "Residual Stress Development during Processing of Graphite/Epoxy Composites," *Comp. Sci. Tech.,* Vol. 36, p.121.

Odian, G., 1991, Principles of Polymerization, 3rd edition, John Wiley & Sons, Inc. New York.

O'Neill, J. M., T. G. Rogers and A. J. M. Spencer, 1988, "Thermally Induced Distortions in the Molding of Laminated Channel Sections, *Math. Eng. Ind.,* Vol. 2, p.65.

Osswald, T.A., "Numerical Methods for Compression Mold Filling Simulation," *Ph.D. Thesis*, Department of Mechanical Engineering, University of Illnois-Urbana Champaign, 1987.

Osswald, T. A. and S. C. Tseng. ,1993, "Orientation and Warpage Prediction in Polymer Processing," a chapter in *Innovation in Polymer Processing.*

Schneider,W., 1971, "Wärmeausdehnungskoeffizienten von Glasfaser-Kunststoff-Verbunden, "Kunststoffe, Vol. 61, p.273.

Simon, S. L. and J. K. Gillham, 1993, "Cure Kinetics of a Thermosetting Liquid Dicyanate Ester Monomer/High-T_g Polycyanurate Material," *J. Appl. Polym. Sci.*, Vol. 47, p.461.

Tseng, S. C., 1993., "Simulation of the Thermomechanical Behavior of Fiber Reinforced Thermoset Composites," Ph.D. *Thesis,* Dept. of Mech. Eng., University of Wisconsin-Madison.

Wisanrakkit, G. and J. K. Gillham, 1990, "The Glass Transition Temperature (T_g) as an Index of Chemical Conversion for High-T_g Amine/Epoxy System: Chemical Diffusion-Controlled Reaction Kinetics," *J. Appl. Polym. Sci.*, Vol. 41, p.2885.